Supporting Information

Soyano et al. 10.1073/pnas.1412716111

SI Materials and Methods

Plasmid Construction. Promoter regions of *CLE ROOT SIGNAL1* (*CLE-RS1*) and *CLE-RS2* were amplified by PCR from MG-20 genomic DNA. The promoter regions were cloned into pENTR-1A (Invitrogen) and then transferred into pMDC162-GFP (1) by LR clonase (Invitrogen). *Pro35S-NODULE INCEPTION* (NIN)-glucocorticoid receptor (GR), *ProNIN-GUS*, and *ProLjUb* (*Lotus japonicus polyubiquitin*)-*NIN-myc* have been described previously (1). For double transformation of roots with promoter-GUS constructs and either *Pro35S-NIN-GR* or its empty vector, *Pro35S-DsRed* was used as the transformation marker for the latter two constructs. Other vectors carried *Pro35S-GFP* as the marker. To analyze NIN-binding nucleotide sequences (NBSs) in *CLE-RS1* and *CLE-RS2* promoters, promoter fragments containing NBSs were amplified by PCR, and cloned upstream of the *CaMV35S* minimal promoter in pENTR-1A-35Smin (1). The resultant chimeric promoters were transferred into pMDC162 (2), pMDC162-GFP (1), and pMDC162-NIN, a pMDC162 derivative, into which *NIN* cDNA was inserted between XhoI sites to replace *HPH* (hygromycin phosphotransferase). Luciferase (LUC) cDNA that was cloned into pENTR-D/TOPO (Invitrogen) was transferred into pUB-GW-GFP (3). Nucleotide sequences of primers used for plasmid construction are listed in Table S1.

Transient Expression Assay in *N. benthamiana* Leaves. *A. tumefaciens* AGL1 transformed with vectors harboring each promoter-GUS reporter and another strain carrying *ProLjUb-LUC* were infiltrated as described by Llave et al. (4). Leaf tissue was harvested at 2.5 d after infiltration. GUS activity was measured as described by Jefferson et al. (5). Tissues (0.2 g) were frozen in liquid nitrogen and homogenized with a tissue lyzer (Quiagen). Protein was extracted with 0.5 mL of extraction buffer (100 mM $NaPO_4$ pH 7.0, 10 mM EDTA, 10 mM β-mercaptoethanol, 0.1% Triton X-100, 0.1% *N*-lauryl-sarcosine, and 0.2 mM PMSF). After centrifugation, 20 μL of the clear supernatant was added into 0.3 mL of extraction buffer containing 20% methanol and 1.4 mM 4-methylumbelliferyl β-D-glucuronide, followed by incubation at 37 °C. Then 50 μL of the reaction mixture was transferred into 0.95 mL of 0.2 M Na_2CO_3 at 0 and 30 min after incubation to stop the reaction. Samples were measured in a microplate reader (SH-9000Lab; Corona) at a 355-nm excitation wavelength and a 460-nm emission wavelength.

For measurement of luciferase activity, 5 μL of the extract was added into 100 μL of LUC assay buffer (20 mM Tricine pH 7.8, 5 mM $MgSO_4$, 0.1 mM EDTA, 5 mM DTT, 150 μM CoA, 250 μM luciferin, and 250 μM ATP). Luminescence was measured in the microplate reader. GUS activities were normalized to those of luciferase.

ChIP-seq Analysis. Chromatin suspensions were prepared from roots transformed with an empty vector and *ProLjUb-NIN-myc.* ChIP was performed with polyclonal anti-myc antibodies (Santa Cruz Biotechnology). Libraries were prepared from three independent ChIP samples according to the instructions for the Illumina ChIP-seq DNA Sample Prep Kit and then sequenced with Hi-seq1000 (Illumina). After sequence reads were trimmed using the FASTX-Toolkit (http://hannonlab.cshl.edu/fastx_toolkit/), 30,922,581 and 52,821,816 reads from empty vector control and NIN-myc, respectively, were mapped to *L. japonicus* genomic sequences using Bowtie 2 (6). MACS2 software (7) with default parameters was used to identify peaks representing enriched binding sites.

1. Soyano T, Kouchi H, Hirota A, Hayashi M (2013) Nodule inception directly targets *NF-Y* subunit genes to regulate essential processes of root nodule development in *Lotus japonicus*. *PLoS Genet* 9(3):e1003352.
2. Curtis MD, Grossniklaus U (2003) A gateway cloning vector set for high-throughput functional analysis of genes in planta. *Plant Physiol* 133(2):462–469.
3. Maekawa T, et al. (2008) Polyubiquitin promoter-based binary vectors for overexpression and gene silencing in *Lotus japonicus*. *Mol Plant Microbe Interact* 21(4):375–382.
4. Llave C, Kasschau KD, Carrington JC (2000) Virus-encoded suppressor of post-transcriptional gene silencing targets a maintenance step in the silencing pathway. *Proc Natl Acad Sci USA* 97(24):13401–13406.
5. Jefferson RA, Kavanagh TA, Bevan MW (1987) GUS fusions: Beta-glucuronidase as a sensitive and versatile gene fusion marker in higher plants. *EMBO J* 6(13):3901–3907.
6. Langmead B, Salzberg SL (2012) Fast gapped-read alignment with Bowtie 2. *Nat Methods* 9(4):357–359.
7. Zhang Y, et al. (2008) Model-based analysis of ChIP-Seq (MACS). *Genome Biol* 9(9): R137.

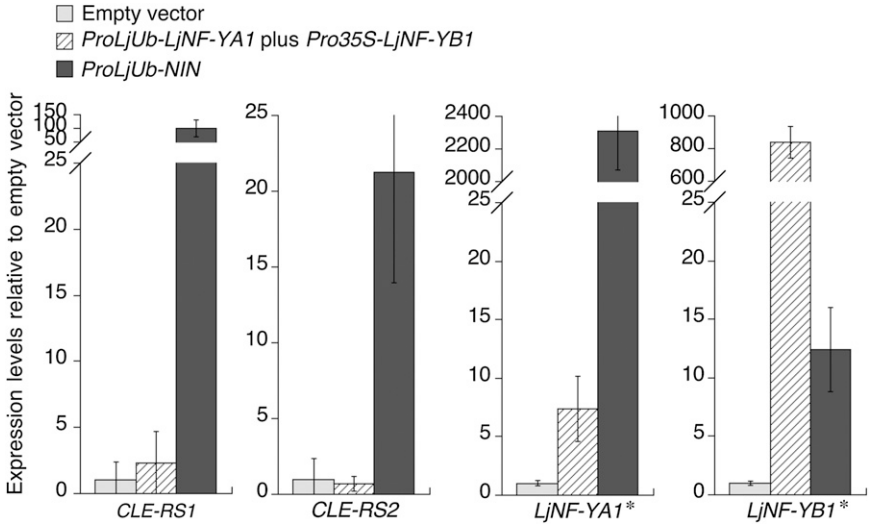

Fig. S1. Expression of *CLE-RS1* and *CLE-RS2* in roots overexpressing *LjNF-YA1* and *LjNF-YB1*. Plants with roots transformed with either an empty vector, *ProLjUb-LjNF-YA1* plus *Pro35S-LjNF-YB1*, or *ProLjUb-NIN* were cultured for 3 wk in the absence of rhizobia. Expression of *CLE-RS1*, *CLE-RS2*, *LjNF-YA1*, and *LjNF-YB1* was analyzed by RT-PCR. Expression levels were normalized using *polyubiquitin* expression. Data are mean ± SD of three biological repeats. Asterisks indicate data from ref. 1.

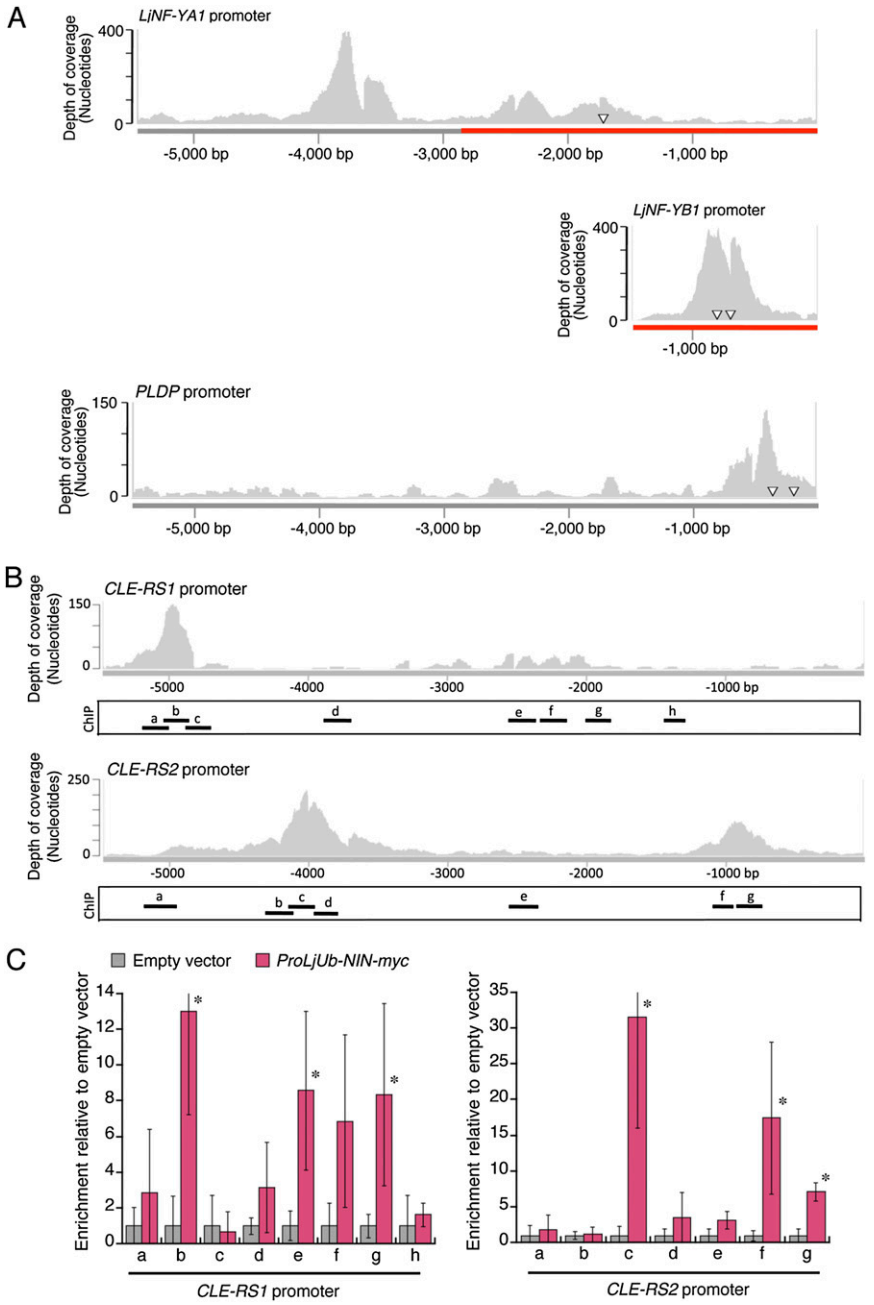

Fig. S2. ChIP-seq analysis of known NIN target genes and ChIP-PCR analysis to confirm binding of NIN with the *CLE-RS1* and *CLE-RS2* promoters. (*A*) Read coverage of *LjNF-YA1*, *LjNF-YB1*, and *Plastocyanin-like domain-containing protein* (*PLDP*) encoding gene promoter regions obtained by the ChIP-seq analysis. Red lines and arrowheads indicate promoter regions and positions of NIN-binding sites used for expression analysis and determined in our previous work (1), respectively. (*B*) Read coverage of the *CLE-RS1* and *CLE-RS2* promoter regions shown in Fig. 2. Regions analyzed by ChIP-PCR are indicated as short bars in boxes. (*C*) ChIP-PCR was performed to examine NIN binding with *CLE-RS1* and *CLE-RS2* promoter regions. DNA fragments were coimmunoprecipitated with polyclonal anti-myc antibodies from chromatin suspensions prepared from *ProLjUb-NIN-myc* roots or control (empty vector) roots. DNA fragments corresponding to regions indicated in *B* were analyzed by RT-PCR. Amounts of DNA fragments were normalized to input data. Data are mean ± SD of three biological repeats. Asterisks indicate significant differences compared with empty vector control roots according to the Student *t* test. $*P < 0.1$.

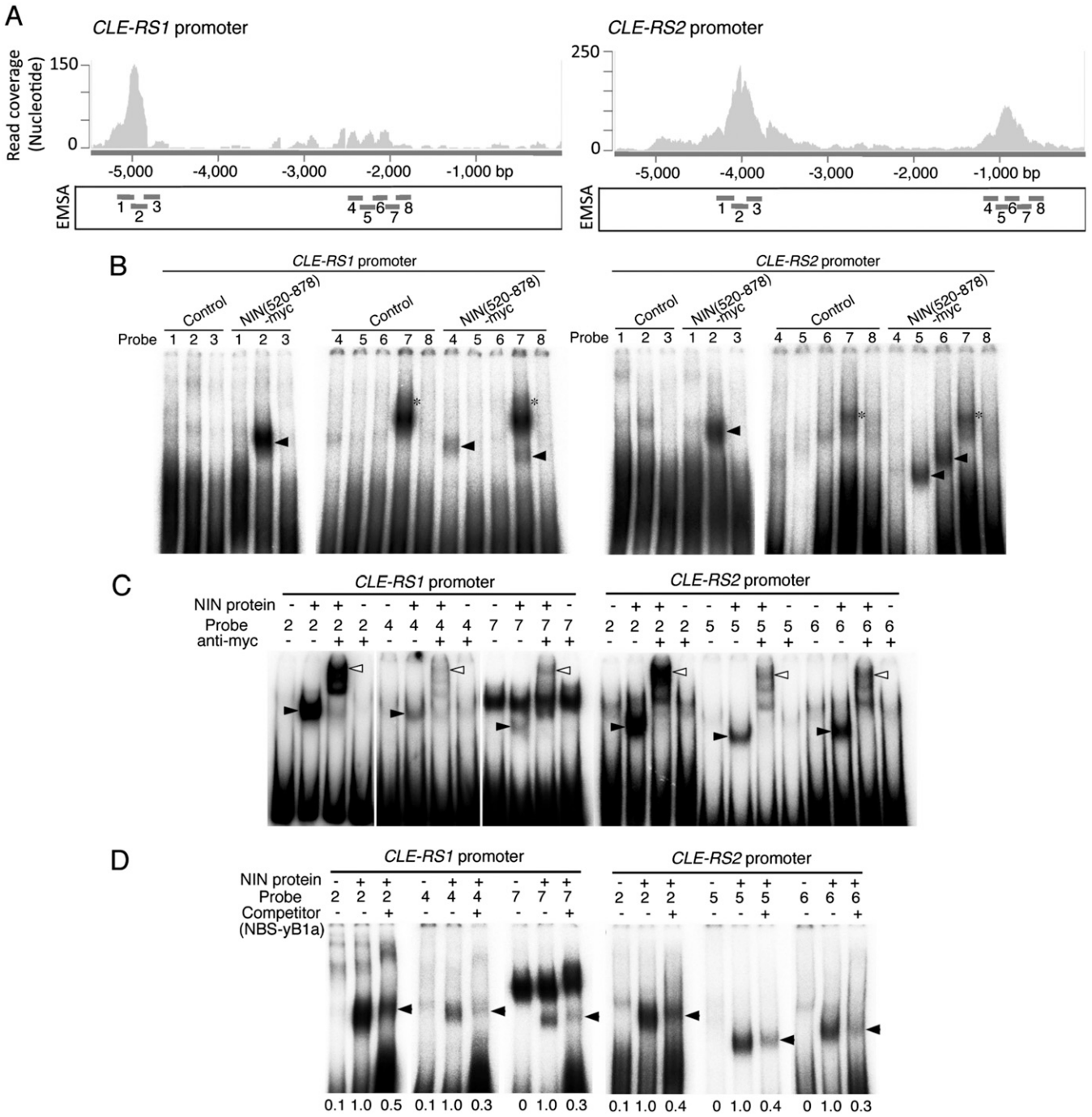

Fig. S3. Specificities of NIN binding with *CLE-RS1* and CLE-*RS2* promoter fragments. (*A*) Read coverage of *CLE-RS1* and *CLE-RS2* promoters obtained by ChIP-seq analysis. Regions corresponding to DNA fragments used for electrophoresis mobility shift assay (EMSA) in *B–D* are indicated as short bars in boxes. The size of the probes are as follows: *CLE-RS1* probe 1, 194 bp; probe 2, 186 bp; probe 3, 184 bp; probe 4, 164 bp; probe 5, 168 bp; probe 6, 170 bp; probe 7, 169 bp; probe 8, 169 bp; *CLE-RS2* probe 1, 203 bp; probe 2, 192 bp; probe 3, 179 bp; probe 4, 166 bp; probe 5, 137 bp; probe 6, 166 bp; probe 7, 173 bp: probe 8, 172 bp. (*B*) EMSA detection of NIN-binding to promoter regions of *CLE-RS1* and *CLE-RS2*. ^{32}P-labeled probes shown in *A* were incubated with NIN(520-878)-myc or in vitro translation products without template (control). Arrowheads and asterisks indicate mobility-shifted bands specifically detected when incubated with the NIN protein and nonspecific bands, respectively. (*C*) Supershift analyses. NIN(520-878)-myc and labeled probes (see *A*) were incubated in the presence (+) or absence (–) of anti-myc antibodies. An in vitro translation product without the template served as a control for the NIN protein. Filled and open arrowheads indicate shifted bands due to NIN binding and supershifted bands, respectively. (*D*) Competition analyses with unlabeled NBS-yB1a. NIN(520-878)-myc and labeled probes were incubated with 200-fold amounts of a competitor, NBS-yB1a, which contains a NBS found in the *LjNF-YB1* promoter (1). Arrowheads indicate shifted bands due to NIN binding. Relative intensities of shifted bands are shown at the bottom.

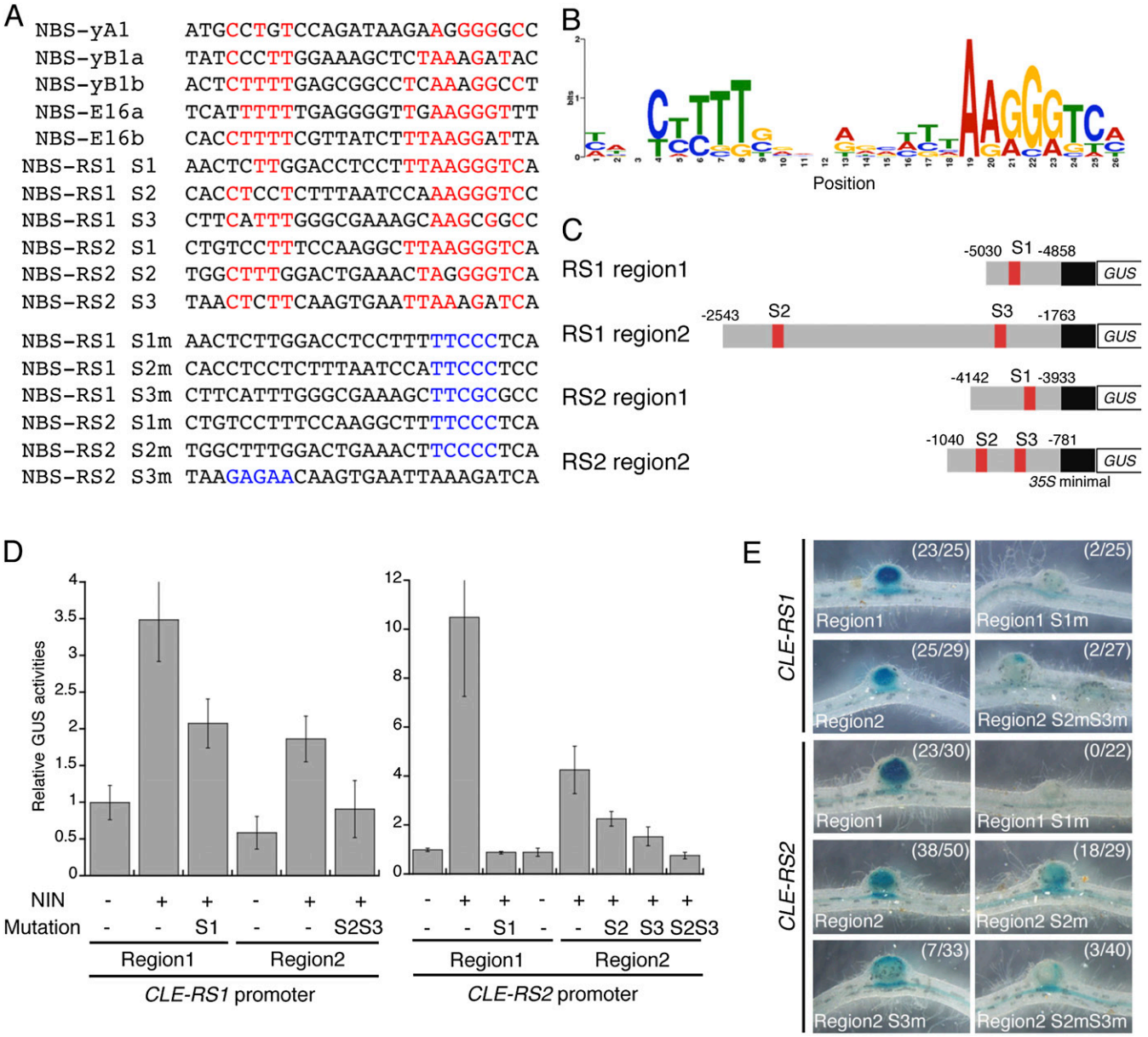

Fig. S4. NBS-dependent transcriptional activation by NIN. (*A*) Alignment of NBSs. NBS-yA1, -yB1a, -yB1b, -E16a, and -E16b have been reported previously (1). NBS-RS1 S1–S3 and NBS-RS2 S1–S3 were identified in the *CLE-RS1* and *CLE-RS2* promoters in this study. NBS-RS1 S1m–S3m and NBS-RS2 S1m–S3m are mutant derivatives. Red characters represent highly conserved nucleotides. Blue characters indicate substituted nucleotides. (*B*) Sequence logo for NBSs aligned in *A*. (*C*) Illustration of promoter-GUS constructs. Promoter fragments containing NBSs from *CLE-RS1* and *CLE-RS2* (gray bars) were inserted upstream of the *CaMV35S* minimal promoter (black bars), followed by the GUS reporter. NBSs are represented as red bars. (*D*) Transient expression assay. *A. tumefaciens* strain carrying a vector harboring each GUS reporter construct and either *Pro35S-NIN* or *Pro35S-HPH* as control and another *Agrobacterium* strain carrying *Pro35S-LUC* were coinfiltrated into *N. benthamiana* leaves. GUS activities in leaf tissues harvested at 2.5 d after infiltration were measured and normalized to those of luciferase. Data are mean ± SD from three biological repeats. (*E*) GUS expression in nodule primordia. Roots transformed with each GUS reporter construct were inoculated with *Mesorhizobium loti*. GUS expression was analyzed at 7 d after inoculation (dai). All samples were incubated in GUS staining buffer for 2 h. The fractions of transformed roots exhibiting GUS expression in nodule primordia are in parentheses.

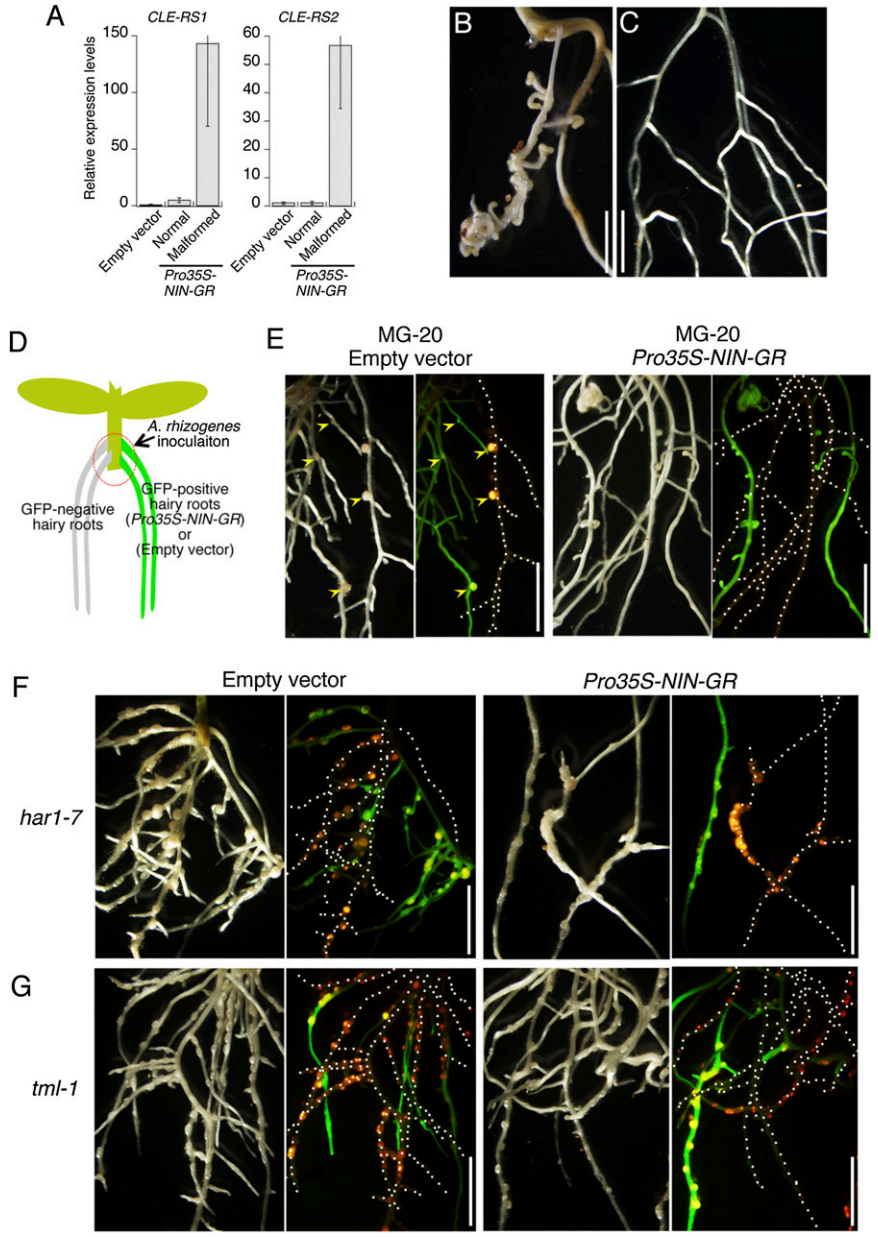

Fig. S5. Expression of *CLE-RS1* and *CLE-RS2* in *Pro35S-NIN-GR* roots, and systemic effects of *NIN* overexpression on nodulation. (*A*) Expression analysis of *CLE-RS1* and *CLE-RS2* in *Pro35S-NIN-GR* roots. Plants with roots that were transformed with the empty vector or *Pro35S-NIN-GR* were cultured for 2 wk in the presence of dexamethasone (DEX). *Pro35S-NIN-GR* roots could be categorized into two groups, malformed roots and roots with normal structure. Expression of *CLE-RS1* and *CLE-RS2* was analyzed by RT-PCR. Expression levels were normalized using *polyubiquitin* expression. Data are mean ± SD of three biological repeats. (*B* and *C*) Roots transformed with *Pro35S-NIN-GR*. Plants were cultured for 3 wk in the presence of DEX and in the absence of rhizobia. A malformed root with the severe phenotype (*B*) and a root with apparently normal architecture (*C*) are shown. (Scale bars: 5 mm.) (*D*) Illustration of the *Agrobacterium*-mediated root transformation. (*E*–*G*) Nodulation on GFP-negative and GFP-positive hairy roots generated in MG-20 (*E*), *hypernodulation aberrant root formation 1-7* (*har1-7*) (*F*), and *too much love-1* (*tml-1*) (*G*) backgrounds. Roots were transformed with *Pro35S-NIN-GR* or the empty vector by the standard *Agrobacterium*-mediated root transformation as illustrated in *D*. (*Left*) Bright-field images. (*Right*) Corresponding fluorescent images with GFP as a transformation marker for roots and DsRed expressed in *M. loti*. Broken lines in the right panels represent GFP-negative roots. Arrowheads in (*E*) indicate infected nodules. Note the absence of nodules in the plant with malformed *Pro35S-NIN-GR* roots. (Scale bars: 5 mm.)

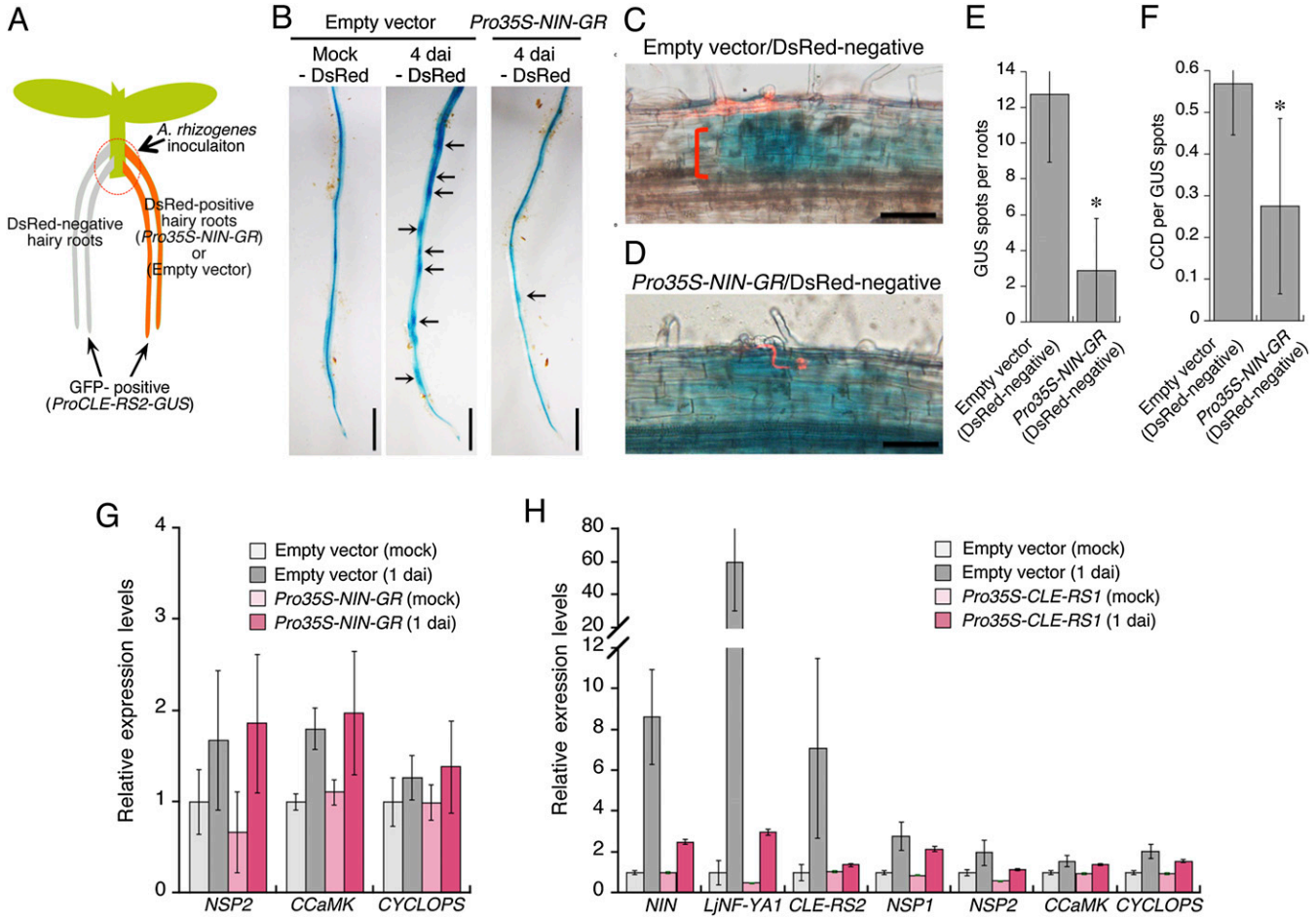

Fig. S6. GUS expression under the *CLE-RS2* promoter and expression of symbiotic genes. (*A*) Illustration of the *Agrobacterium*-mediated double-root transformation. Roots were cotransformed with *ProCLE-RS2-GUS* and either the empty vector or *Pro35S-NIN-GR*. The former reporter construct carried *Pro35S-GFP* as a transformation marker; the latter two constructs carried *Pro35S-DsRed*. (*B*) Histochemical GUS staining analysis. Roots were transformed as illustrated in *A*. Plants (Gifu B-192) were inoculated in the presence (4 dai) or absence of *M. loti* for 4 d (mock) after 5 d of treatment with DEX. GUS expression from the *CLE-RS2* promoter was observed in DsRed-negative roots (−DsRed). Arrows indicate GUS staining spots. (Scale bars: 1 mm.) (*C* and *D*) Magnified images of GUS staining spots in DsRed-negative control roots (*C*) and DsRed-negative roots of plants with malformed *Pro35S-NIN-GR* roots (*D*). Divided cortical cells can be seen in *C* as indicated by the red bar. DsRed fluorescence indicating infection foci of DsRed-labeled *M. loti*. (Scale bars: 50 μm.) (*E* and *F*) Number of GUS staining spots (*E*) and ratios of GUS spots containing divided cortical cells (*F*). Mean ± SD numbers ($n > 25$) in DsRed-negative control roots and DsRed-negative roots of plants that also generated malformed *Pro35S-NIN-GR* roots are shown. The numbers of GUS spots in areas 2 cm from root tips were counted. Asterisks indicate significant differences compared with DsRed-negative control roots according to the Student *t* test. *$P < 0.01$. (*G* and *H*) Expression of symbiotic genes in roots. (*G*) Plants generated roots that were transformed with an empty vector or *Pro35S-NIN-GR* were grown for 5 d in the presence of DEX, and then inoculated with (1 dai) or without (mock) *M. loti*. Transformed roots were distinguishable by fluorescence of the DsRed transformation marker. Gene expression in DsRed-negative control roots and DsRed-negative roots of plants that also generated DsRed-positive *Pro35S-NIN-GR* roots was analyzed by RT-PCR. (*H*) Expression of symbiotic genes in roots transformed with the empty vector or *Pro35S-CLE-RS1* was analyzed at 1 dai with (1 dai) or without (mock) *M. loti*. Expression levels were normalized to *polyubiquitin* expression. Data are mean ± SD of three biological repeats.

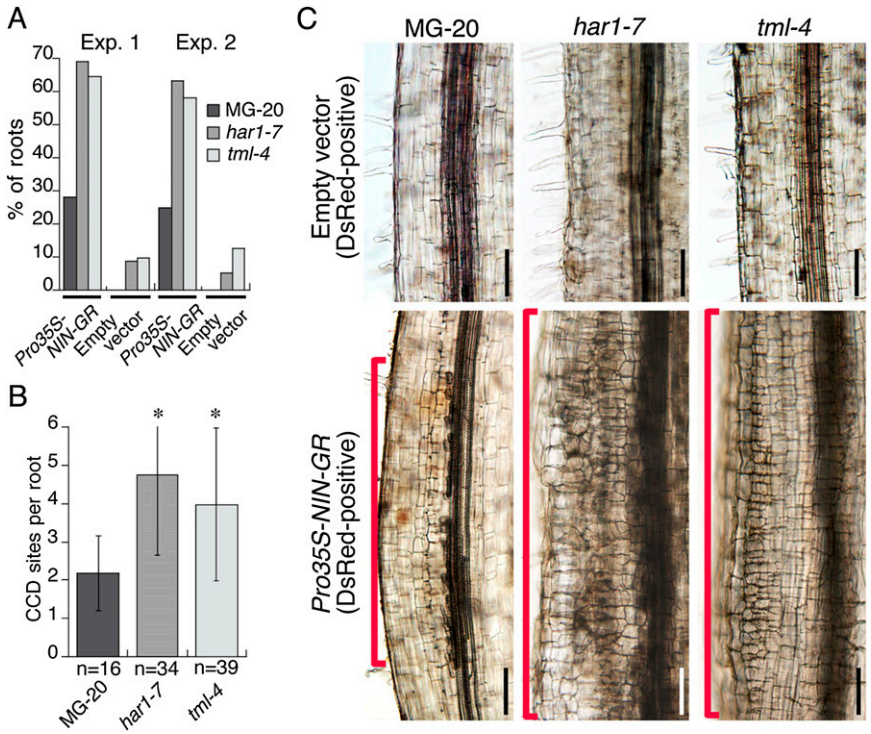

Fig. S7. Cortical cell divisions induced by *NIN* overexpression in *har1* and *tml* mutants. (*A*) Proportions of DsRed-positive *Pro35S-NIN-GR* roots with ectopic cortical cell division in two independent experiments. More than 25 roots were analyzed in each line. (*B*) Mean ± SD numbers of sites where cortical cell division occurred in DsRed-positive *Pro35S-NIN-GR* roots. Asterisks indicate significant differences from MG-20 according to the Student *t* test ($P < 0.01$). (*C*) Ectopic cortical cell division in transformed roots. Plants with roots transformed with the empty vector or *Pro35S-NIN-GR* were cultured for 3 wk after being transferred to soil supplemented with DEX. Red bars indicate regions in which cortical cell division occurred. (Scale bars: 100 μm.)

Other Supporting Information Files

Table S1 (DOCX)
Dataset S1 (XLSX)